Slowing down of light pulses using photorefractive four-wave mixing: Nontrivial behavior with increasing coupling strength

Konstantin Shcherbin,[1,*] Pierre Mathey,[2] Grégory Gadret,[2] Romain Guyard,[2] Hans Rudolf Jauslin,[2] and Serguey Odoulov[1]

[1]*Institute of Physics, National Academy of Sciences, Prospekt Nauki 46, 03028 Kiev, Ukraine*

[2]*Laboratoire Interdisciplinaire Carnot de Bourgogne, UMR 6303 CNRS-Université de Bourgogne, 9 Avenue Alain Savary, BP 47870, 21078 Dijon Cedex, France*

(Received 9 November 2012; published 18 March 2013)

The slowing down of light pulses with backward-wave four-wave mixing is analyzed for photorefractive crystals with different coupling strengths. The conditions are found for which the delay of a phase-conjugate pulse decreases when the coupling strength increases and can even become negative, switching the pulse deceleration to acceleration. It is shown that for relatively low coupling strength the backward-wave four-wave mixing ensures a longer delay as compared to the two-beam-coupling technique. For coupling strengths tending to zero, the delay of long pulses approaches the response time of the medium. The conclusions of the theoretical analysis are confirmed experimentally with backward-wave four-wave mixing in barium titanate.

DOI: 10.1103/PhysRevA.87.033820 PACS number(s): 42.65.Hw, 42.70.Nq, 42.81.Dp

I. INTRODUCTION

It has been known for more than a century [1,2] that the group velocity v_{gr} of light in dispersive media can be less than or greater than the phase velocity $v_{ph} = c/n$ (where c is the phase velocity of light in vacuum and n is the refractive index) and that it can even become negative. Light pulses can therefore be decelerated or accelerated when propagating through the medium. Interest in this phenomenon was revitalized when a considerable deceleration of light pulses was achieved using electromagnetically induced transparency (EIT) [3,4] at the end of the last century. Slow and fast light attract much attention because of their potential applications [5,6] that include, among others, optical delay lines [7], high-sensitivity interferometry [8] and sensors [9], radio-frequency phase shifters [10], gigahertz-bandwidth atomic probes [11], etc.

Large dispersion is necessary to achieve a noticeable change in the group velocity. This can be natural dispersion related to the resonances of atoms, molecules, or collective excitations in solid states, but more interesting are nonlinear effects where the light itself creates new resonances with sufficiently large dispersion. A perfect example is the EIT technique [3,4] where a narrow dip in a strong absorption band may be created by precise frequency adjustment of two coherent light waves in a three-level atomic system (lambda system). The typical half-width of the induced transparency window in an ultracold gas of sodium atoms is about 1 MHz; such a narrow resonance allows for achieving a group velocity of 32 m/s with 2.5-μs-long light pulses [4].

The other attractive possibility consists of using resonances of different three-dimensional (3D) structures imprinted or created by light in material. Boyd named such techniques "structural slow light," [12] having in mind first of all permanent structures like photonic bandgap crystals of different types. The dynamic structures that light can itself create may also be very promising. Quasistatic index gratings have been considered, which appear when two or several light beams are mixed nonlinearly in the bulk of a photorefractive material [13] or in different light valves made, for example, by the association of a nematic liquid crystal layer and a photorefractive crystal [14].

The dynamic photorefractive gratings that were used for pulse deceleration provide Bragg resonances with half-width of a fraction of a Hz [13]; consequently, the group velocity of 0.025 cm/s was demonstrated. The main advantages of the photorefractive techniques are that they do not need precise frequency adjustment and it is possible to work at ambient temperatures and within a broad spectral range. It should be noted, however, that only long pulses, with full width at half maximum (FWHM) on the order of 1 s could be delayed in Ref. [13] with such a small group velocity with no distortion of the temporal envelope. Thus, slow light with traditional ferroelectric photorefractive crystals is useful first of all for the modeling different wave-mixing geometries [13–16]; the practical results may bring semiconductor photorefractives that possess much faster nonlinearities [17,18].

This is not, however, the only field for photorefractive light-pulse manipulation. The possibility to govern in a controllable way the additional dispersion (even with a relatively slow response) may find applications in polarization interferometry [19] and in systems where special dispersion profiles should be tailored. An interesting application discussed in Ref. [20] is related to a problem of a "white light interferometer" necessary for gravitational-wave detection. The possibility to control the dispersion spectrum becomes here of primary importance; at the same time it is important also for controlling the pulse delay time.

The first implementations of the dynamic phase gratings for pulse manipulation [13] were based on two-beam coupling in crystals with the diffusion-driven charge transport. The effect of such a coupling on the transmitted signal beam is similar to that of an amplifier with limited bandwidth. The amplitude transmission for the signal wave A_S is

$$T(\Delta\omega) = \frac{A_S(d)}{A_S(0)} = \exp[\gamma(\Delta\omega)d], \tag{1}$$

with the interaction length d, frequency detuning of the signal with respect to the pump $\Delta\omega$, and complex coupling constant

*kshcherb@iop.kiev.ua

 ©2013 American Physical Society

$\gamma(\Delta\omega)$. The real part of $\gamma(\Delta\omega)$ is Lorentzian in shape and the imaginary part has a dispersive profile. This similarity of two-beam coupling to the amplifier with an isolated spectral line results in a similarity of the observed effects. The pulse, with a Gaussian temporal envelope, is amplified and delayed in time. Both the gain in intensity and the pulse deceleration scale with coupling strength γd. It is important that the spectral profile of the complex transmission function $T(\Delta\omega)$ is independent of γd.

The situation is more complicated for photorefractive backward-wave four-wave mixing (BWFWM) [21–24] because not only the magnitudes but also the spectral profiles of the transmission and phase-conjugate reflectivity vary with the coupling strength [25–27]. With increasing coupling the spectrum of the phase conjugate reflectivity may change dramatically from bell shaped to a spectrum possessing two maxima located symmetrically with respect to zero frequency detuning. The phase-coupling spectrum, which represents in fact the dispersion for the phase-conjugate wave, is modified, too.

In the present paper we qualitatively analyze such transformations of the spectral profiles with the aim to find the peculiarities and advantages of photorefractive BWFWM for reducing the speed of light pulses. The emphasis is put on uncommon behavior when the speed reduction of pulse propagation decreases with increasing coupling strength. The temporal manipulation of light pulses is studied first numerically and then confirmed experimentally for different coupling constants and pump intensity ratios with a classical photorefractive crystal, $BaTiO_3$.

II. THEORETICAL BACKGROUND

A. Spectral dependencies of phase-conjugate reflectivity and phase of conjugate wave

In the photorefractive two-beam coupling configuration the signal beam 4 and one pump beam 1 interfere in the photorefractive crystal as shown in Fig. 1(a) by black lines. This results in the recording of a refractive-index grating. The grating recorded by diffusion-charge transport is $\pi/2$ $(-\pi/2)$ shifted with respect to the interference pattern. The pump beam diffracts from the grating with a given diffraction efficiency and its diffracted part interferes with the transmitted part of the signal wave, thus giving rise to an amplification (attenuation) of the signal 4. If a second pump 2 impinges on the crystal from the direction opposite to pump 1, the diffraction of this second pump from the grating gives rise to the appearance of a back-propagating beam 3. Wave 3 is the phase-conjugate replica of the signal wave 4 for a pair of pump waves (1, 2) with mutually conjugated wavefronts [28,29]. This interaction may occur in media with different optical nonlinearities and is denoted as backward-wave four-wave mixing (BWFWM). We consider in what follows the recording of nonlocal transmission gratings only, i.e., the phase-conjugate beam 3 appears as a result of the diffraction of pump 2 from the grating recorded by beams 4 and 1. Generally, theory [30] predicts qualitatively similar results for the recording of only a transmission grating, only a reflection grating, or both transmission and reflection gratings simultaneously within the approximation of nonabsorbing crystal and undepleted pumps.

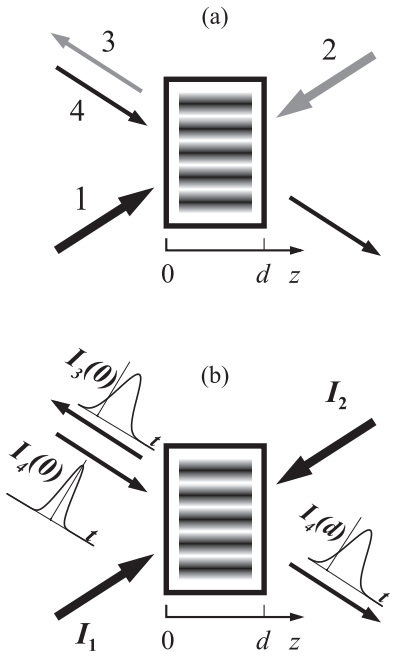

FIG. 1. (a) Schematic representations of BWFWM configuration and (b) input-output pulses in the experiments on light pulses slowing down. Two counter-propagating pump waves 1 and 2, signal wave 4, and conjugate wave 3 have the amplitudes A_1, A_2, A_3, A_4 and the intensities I_1, I_2, I_3, I_4, respectively.

The spectral response of the phase-conjugate reflectivity is determined as [25]

$$\rho(\Delta\omega) = \frac{A_3(0,\Delta\omega)}{A_4^*(0,\Delta\omega)} = \frac{\sinh\left(\frac{\Gamma_\omega}{2}\right)}{\cosh\left(\frac{\Gamma_\omega}{2} + \frac{\ln r}{2}\right)} = |\rho(\Delta\omega)|\exp[-i\varphi(\Delta\omega)], \quad (2)$$

where $\Gamma_\omega = \gamma d/(1 - i\Delta\omega\tau)$ is the rate coefficient for the wave amplitudes, the complex coupling constant γ is real for photorefractive crystals with nonlocal response, τ is the response time and $r = I_2(d)/I_1(0)$ is the pump intensity ratio. The normalized amplitude of the phase-conjugate wave and its nonlinear phase shift are $|\rho(\Delta\omega)|$ and $\varphi(\Delta\omega)$, respectively. The frequency dependence of the phase shift $\varphi(\Delta\omega)$, which is due to self-diffraction from the photorefractive grating, acts as the dispersion of a medium and slows down the light pulses. The standard relation that links the phase and the group velocity $v_{gr} = c/(n + \omega dn(\omega)/d\omega)$ derived by Rayleigh for acoustic waves [31] may be written for the phase-conjugate wave in the following form:

$$v_{gr}(\Delta\omega) = \frac{c}{n + c\frac{d\varphi\prime(\Delta\omega)}{d\Delta\omega}} \approx \frac{1}{d\varphi\prime(\Delta\omega)/d\Delta\omega}, \quad (3)$$

where $\varphi'(\Delta\omega)$ is the phase shift per unit length and n is an unperturbed value of the refractive index.

If compared with the transmission for two-beam coupling [see Eq. (1)], the BWFWM reflectivity is a more complicated function. First, it includes a new parameter: the pump ratio. Second, the spectral profiles of $\rho(\Delta\omega)$ are obviously dependent on the coupling strength. As a consequence, the derivative $d\varphi'(\Delta\omega)/d\Delta\omega$ that defines group velocity in Eq. (3) becomes

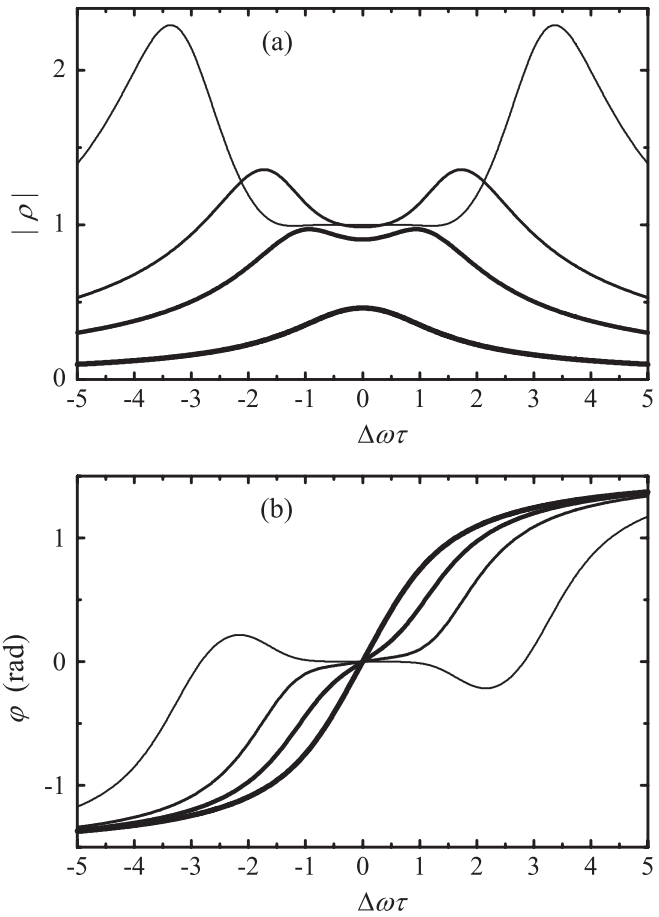

FIG. 2. (a) Spectra of normalized amplitude $|\rho|$ and (b) phase shift φ of the phase-conjugate wave in dimensionless-frequency coordinates $\Delta\omega\tau$, calculated according to Eq. (2) for $r = 1$ and coupling constant $\gamma d = -1, -3, -5, -10$ from thickest to thinnest line, respectively.

dependent on coupling strength, too, and can even change its sign with the increase of γd, as shown below.

The spectral profiles of the amplitude and the phase of the phase-conjugate reflectivity calculated from Eq. (2) for $r = 1$ and for coupling constants $\gamma d = -1, -3, -5, -10$ are shown in Figs. 2(a) and 2(b). The negative sign for the coupling constant corresponds to the experimental geometry where the transmitted beam 4 is amplified while the phase-conjugate beam 3 is attenuated. It should be noted that the spectra are exactly the same if we change simultaneously $\gamma d = -\gamma d$ and $r = 1/r$, according to the general properties of the theoretical model [25].

The formation of the spectra with two maxima for the phase conjugate reflectivity [Fig. 2(a)] at sufficiently high coupling strength was already known long ago [26]. The object of our main interest is the spectrum of nonlinear phase that the wave acquires when being conjugated [Fig. 2(b)]. For small γd the dependence $\varphi(\Delta\omega)$ is a smooth curve with the largest derivative $d\varphi(\Delta\omega)/d\Delta\omega$ at $\Delta\omega = 0$. With increasing coupling strength it starts to deform: the slope of the curves (derivative) diminishes but always remains positive for the detuning range close to zero while the large slope is observed at higher-frequency detuning. This tendency holds with still increasing coupling strength until peculiarities with local extrema appear at a certain critical γd. Obviously the intervals with negative derivative $d\varphi(\Delta\omega)/d\Delta\omega$ appear between extrema and zero frequency detuning. According to Eq. (3) the decrease of the derivative predicts a group velocity approaching c and consistent diminishing of the pulse delay with rising coupling strength. Moreover, the appearing intervals with negative slope suggest that the pulse delay may be switched to pulse acceleration if the spectral content of the pulse correspond to these intervals.

The predicted inhibition of beam deceleration with increasing coupling strength and switching from deceleration to acceleration are rather unexpected effects and might even be considered counterintuitive. Except for the nonlocal photorefractive nonlinearity, practically for all other nonlinear effects used for pulse manipulation the deceleration (or acceleration) increases with the increasing coupling. A clear look, however, shows no paradox here. The phase-conjugate reflectivity $\rho(\Delta\omega)$ increases at $\Delta\omega = 0$ with coupling strength and goes asymptotically to unity for the chosen pump ratio $r = 1$. At the same time, starting from a certain coupling strength, $\rho(\Delta\omega)$ may grow faster at shifted frequencies $\Delta\omega \neq 0$ and considerably exceed unity.

The qualitative explanation for the above-described deformations of phase conjugate reflectivity spectra is as follows: Because of the specific nonlocal type of photorefractive nonlinearity, the two index gratings (one recorded by the signal wave 4 with the pump wave 1 and the other recorded by the pump wave 2 with the phase-conjugate wave 3) are shifted $\pi/2$ with respect to the interference fringes but the shift for different gratings is in different directions. This is why the sum shift of these gratings with respect to each other appears to be strictly π in the degenerate case with $\Delta\omega = 0$. A quite strong compensation of the overall index modulation occurs and the growth of the phase-conjugate reflectivity is inhibited. The compensation is especially strong for equal intensities of the pump waves, $r = 1$. Any frequency detuning of the signal wave results in motion of the interference fringes. This motion, in turn, causes additional phase shift of the index gratings because of the finite response time of the material. As a result the exact destructive superposition of the gratings recorded by pairs of co-propagating waves becomes broken. The phase-conjugate reflectivity may therefore grow further at $\Delta\omega \neq 0$, exceed 1, and additional maxima may be formed for sufficiently large coupling strengths [26]. The development of the reflectivity spectrum with two maxima is accompanied by the corresponding changes in the dispersion described above. The changes in dispersion curves with increase of the coupling strength may result in decrease of the delay for the conjugate pulse.

B. Calculation of delay for phase-conjugate and transmitted pulses

The transformation of an input pulse $I_4(0,t)$ with a Gaussian temporal profile into a transmitted pulse $I_4(d,t)$ and a phase-conjugate pulse $I_3(0,t)$, which is due to BWFWM with two continuous-wave (cw) pump waves 1 and 2 [see Fig. 1(b)], is considered below. The theory [21,22] gives the Fourier components of the conjugate-wave amplitude $\tilde{A}_3^*(0, \Delta\omega)$ and

transmitted wave amplitude $\tilde{A}_4(d, \Delta\omega)$ expressed in terms of the Fourier component of the input signal $\tilde{A}_4(0, \Delta\omega)$:

$$\tilde{A}_3^*(0, \Delta\omega) = \sqrt{r}\exp(-i\phi)\frac{1-\exp(\Gamma_\omega d)}{1+r\exp(\Gamma_\omega d)}\tilde{A}_4(0, \Delta\omega), \quad (4)$$

$$\tilde{A}_4(d, \Delta\omega) = \frac{(1+r)\exp(\Gamma_\omega d)}{1+r\exp(\Gamma_\omega d)}\tilde{A}_4(0, \Delta\omega), \quad (5)$$

where the phase $\phi = \arg(A_1 A_2)$ is constant in the undepleted-pump approximation and the asterisk indicates complex conjugation. For a Gaussian-shaped input pulse $A_4(0, t) = A_4^0\exp(-t^2/2t_0^2)$ with t_0 being the half-width of the pulse intensity at $1/e$, the Fourier transform $\tilde{A}_4(0, \Delta\omega)$ also has a Gaussian profile $\tilde{A}_4(0, \Delta\omega) = (A_4^0 t_0/\sqrt{2\pi})\exp(-\Delta\omega^2 t_0^2/2)$. The temporal dependencies of the output pulse amplitudes $A_3(0,t)$ and $A_4(d,t)$ can be calculated from Eqs. (4) and (5) using the inverse Fourier transform. Then the delay Δt of the pulse maximum, which we use to characterize the reduction in speed, can be evaluated from the temporal envelopes of the output pulses.

The solid and dotted lines in Fig. 3 represent the coupling-strength dependencies of the delay of the pulse maximum for the phase-conjugate $I_3(0,t)$ and transmitted $I_4(d,t)$ pulses, respectively, calculated for an input pulse with the dimensionless pulse half-width $t_0/\tau = 2.7$ and for pump beam ratios $r = 1$, 0.06, and 0.006. The calculation of the delay for the transmitted pulse in the two-beam-coupling configuration is shown by a dashed line for comparison.

Two important conclusions follow from the dependencies in Fig. 3. The first is the obvious difference in the delay for the conjugate and transmitted pulses for $\gamma d \to 0$. This difference is explained by different origin of the output pulses. Similarly to the single output of the two-beam-coupling scheme, the transmitted beam 4 results from the interference between the part of the input signal 4 transmitted through the crystal with no coupling and the components diffracted from the pump 1 in the direction of beam 4. It is evident that for a zero-coupling constant there is no nonlinear interaction, there is no diffracted component, and the delay of the transmitted pulse is zero.

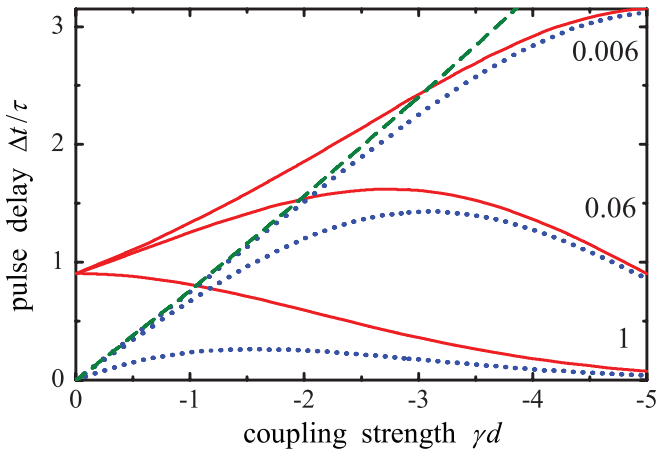

FIG. 3. (Color online) Temporal delay of pulse maximum versus coupling strength for phase-conjugate $I_3(0,t)$ (solid lines) and transmitted $I_4(d,t)$ (dotted lines) pulses, calculated for input pulse half-width $t_0/\tau = 2.7$ and for beam ratios $r = 1$, 0.06, and 0.006. The dashed line represents the calculation for two-beam coupling.

On the contrary, the phase-conjugate pulse results from the diffraction of the pump wave from the photorefractive grating but it does not contain any part of the linearly transmitted signal. Even being very weak, the grating is built with the response time of the medium. The inertia of the medium introduces a delay in the phase-conjugate beam. There is no phase-conjugate pulse for $\gamma d = 0$ and the delay, therefore, is not defined. However, the delay for this pulse starts from a nonzero value for $\gamma d \to 0$. It exceeds the delay of the transmitted pulse in BWFWM and, for relatively small coupling strengths ($|\gamma d| < 2$ for $r = 0.06$), also in two-beam coupling.

The second important conclusion is that the delay of the phase-conjugate pulse for large pump ratios decreases with increasing coupling strength $|\gamma d|$, as expected from the phase-coupling spectra shown in Fig. 2(b). For small pump ratios the decrease is observed also, but after a maximum which is reached at larger absolute values of the coupling constant. The delay of the transmitted beam initially increases with $|\gamma d|$ for any r, passes the maximum, and diminishes, similarly to the delay of the phase-conjugate pulse when the component diffracted from the pump dominates in the overall transmitted wave.

For the pulsed recording regime, the grating reaches its steady state with long pulses when $t_0 > \tau$. The maximum absolute delay is achieved in this case. To characterize the delay of the phase-conjugate pulse for $\gamma d \to 0$, this delay is calculated as a function of the input pulse half-width t_0/τ. The result for $\gamma d = -10^{-10}$ is shown in Fig. 4. It is evident that for a long-pulse recording the delay of the phase-conjugate pulse tends to the response time of the crystal. It should be noted that this result does not depend on the pump-beam ratio: the curves for different r are the same because the nonlinear coupling between the optical waves is negligible at any r. The calculation for $\gamma d = -2.8$ and $r = 1$ is presented in Fig. 4 for comparison.

For a given coupling constant the maximum phase-conjugate reflectivity is achieved at an optimum pump beam ratio $r_{\text{opt}} = \exp(\gamma d)$ [25]. The delay of the conjugate pulse as a function of coupling strength, calculated for each optimum pump ratio (solid line) is compared in Fig. 5 with the delay of

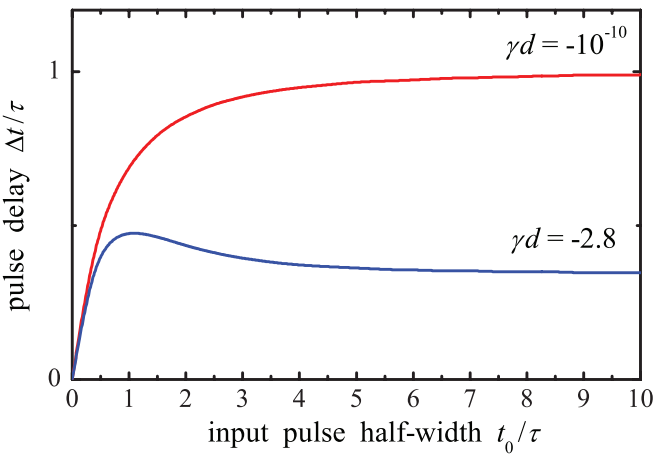

FIG. 4. (Color online) Temporal delay of maximum versus input pulse half-width for phase-conjugate pulse $I_3(0,t)$, calculated for $r = 1$ with $\gamma d = -10^{-10}$ and $\gamma d = -2.8$.

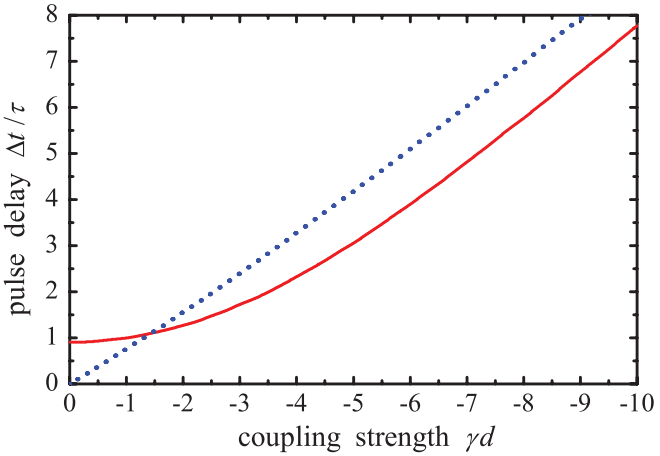

FIG. 5. (Color online) Temporal delay of maximum versus coupling strength for phase-conjugate pulse calculated with an optimal beam ratio (solid line) and for the transmitted pulse in the two-beam-coupling configuration (dots), both computed for $t_0/\tau = 2.7$.

the transmitted pulse in the two-beam-coupling scheme (dotted line). For both curves the input pulse half-width is $t_0/\tau = 2.7$. The delay of the phase-conjugate pulse in BWFWM is longer until the coupling strength reaches $\gamma d \approx -1.4$. It should be noted that for a large $|\gamma d|$ the beam ratio $r < r_{\text{opt}}$ can be chosen, which ensures almost the same delay as the two-beam-coupling scheme with still sufficiently high phase-conjugate reflectivity.

The calculated spectra of the nonlinear phase shift for the phase-conjugate wave [Fig. 2(b)] show that for a large coupling strength $|\gamma d|$ the slope of $d\varphi(\Delta\omega)/d\Delta\omega$ changes its sign within a certain frequency interval. This indicates according to Eq. (3) that the reduction in speed of the pulse with a certain spectrum is switched to acceleration, with Δt becoming negative. It should be noted here that in a very narrow range of detunings in the vicinity $\omega\tau = 0$ the slope is always positive; the wings with negative slope that may ensure pulse acceleration appear at nonzero frequency.

The negative delay with a small magnitude is calculated for the data presented in Fig. 3 for $r = 1$ and $|\gamma d| > 7$. For the observation of a net switching from the delay to acceleration the spectral content of the input pulse should correspond to the spectral range where wings with a negative slope appear in Fig. 2(b). To find the proper pulse duration, the delay for the phase-conjugate pulse is calculated as a function of the input pulse half-width for $\gamma d = -10$ and $r = 1$, shown by a solid line in Fig. 6. The detailed study shows that the delay becomes positive again for $t_0/\tau > 5$ and then approaches $\Delta t/\tau \approx 10^{-3}$ (see inset in Fig. 6). The positive delay for very long pulses is in agreement with the phase-shift spectrum calculated in Fig. 2(b) where the slope of the dependencies is always positive in the vicinity of $\Delta\omega = 0$.

The largest pulse acceleration calculated in Fig. 6 appears for the input pulse half-width $t_0/\tau \approx 1.1$. To analyze the transition from the pulse slowing down to the acceleration with the change of the coupling strength, the position of the phase-conjugate pulse maximum is calculated as a function of γd for $r = 1$ and $t_0/\tau = 1.1$ (solid line in Fig. 7). The delay of the phase-conjugate pulse at first decreases with the coupling

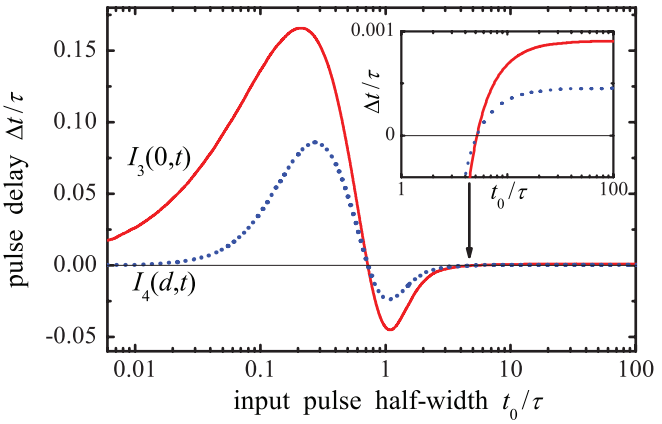

FIG. 6. (Color online) Temporal delay of maximum versus input pulse half-width for the phase-conjugate $I_3(0,t)$ and transmitted $I_4(d,t)$ pulses, calculated for $r = 1$ and $\gamma d = -10$; inset represents the same data in different scales.

strength $|\gamma d|$, similarly to the results shown in Fig. 3 for $r = 1$ and $t_0/\tau = 2.7$, then passes zero at $\gamma d \approx -7.5$, reaches its maximum negative value and further returns to zero. The study in a large scale indicates that the delay exhibits dumped oscillations around zero with the increasing $|\gamma d|$ (see inset of Fig. 7). The variation of the delay of transmitted pulse $I_4(d,t)$ behaves similarly to that of the phase-conjugate pulse $I_3(0,t)$ but with a smaller magnitude (see dots in Figs. 6 and 7). A considerable part of beam $I_4(d)$ is a zero-order diffraction from the incident signal pulse $I_4(0)$, which explains a less-pronounced effect in the transmitted beam.

III. EXPERIMENTAL VERIFICATION

A cobalt-doped barium titanate crystal ($BaTiO_3$) is used in the experiment as a nonlinear medium. Two cw counter-propagating pump beams 1 and 2 from an Ar^+ laser (TEM_{00}, single frequency, $\lambda = 514$ nm, total power $\sim$200 mW) enter the sample as shown in Fig. 1(b). A weak signal beam $I_4(0)$ with an intensity of the order of 10^{-5} of the total pump intensity

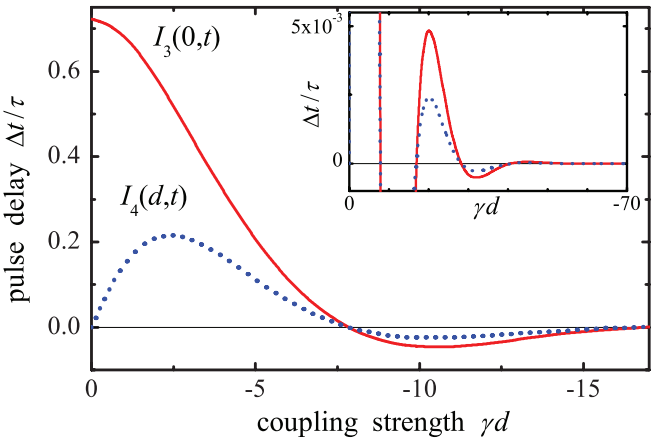

FIG. 7. (Color online) Temporal delay of maximum versus coupling strength for phase-conjugate $I_3(0,t)$ and transmitted $I_4(d,t)$ pulses calculated for $r = 1$ and $t_0/\tau = 1.1$; inset represents the same data in different scales.

impinges on the sample at the angle of $2\theta \approx 20^\circ$ with respect to the pump I_1 (grating spacing $\Lambda \approx 1.4\ \mu$m). All the beams are polarized initially in the plane of incidence. The path difference between the three incident beams is chosen so that beam I_2 is not coherent with the two mutually coherent beams I_1 and I_4. This ensures the recording of the transmission gratings only. The input z face of the crystal is tilted in the plane of incidence by nearly 30° with respect to the bisecting line between recording beams I_1 and I_4 to benefit from the largest component r_{42} of the electro-optic tensor of $BaTiO_3$ [32].

The response time $\tau = 2.3$ s of the crystal for a total intensity of 11 W/cm^2 is measured in two-beam-coupling configuration with pump I_2 blocked. The coupling strength is estimated from the optimal pump ratio [25] at which the largest phase-conjugate reflectivity is reached with the cw beam $I_4(0)$ to be $\gamma d = \ln(r_{\text{opt}}) = \ln(0.06) \approx -2.8$.

The coupling strength is controlled in the experiment by changing the polarization of all recording beams. For evaluation of the coupling strength dependence on the polarization, the amplification of the transmitted beam $I_4(d)$ is measured with a conventional two-beam-coupling configuration with a cw input $I_4(0)$ and with no pump I_2. The coupling strength γd is deduced from the two-beam-coupling gain factor Γ as $\gamma d = -\Gamma d/2$. The dependence of the coupling strength γd on the recording-beam polarization is shown in Fig. 8. Using these data, the correspondence between the light polarization and the coupling strength is established.

A larger coupling strength can be achieved with our sample by increasing the tilt of the crystal. The comparison of the delayed pulses measured for different large coupling strengths become difficult, however. The difficulty relates to the dependence of the photorefractive response time on photoconductivity and therefore on the light intensity. The intensity in the interaction area decreases at large coupling strength because a large power of the pump beams is scattered into beam fanning. Consequently, the response time decreases and all the delay characteristics are changed accordingly. This makes difficult a correct comparison of the dependencies measured for different coupling strength. To overcome this problem we limit the coupling strength in the experiments to $|\gamma d| = 2.8$ at which the effect of beam fanning is still not crucial.

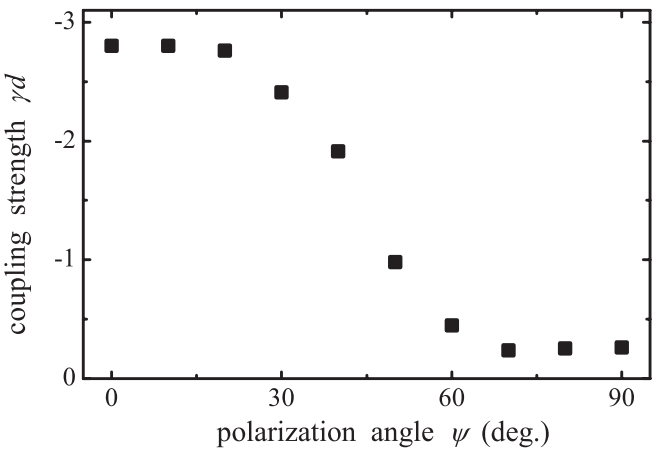

FIG. 8. Coupling strength as a function of polarization of the recording beams $I_4(0)$ and $I_1(0)$ measured in a two-beam-coupling experiment.

In the experiments on pulsed recording, the Gaussian temporal profile of the input pulse $I_4(d = 0, t) = I_4^0 \exp(-t^2/t_0^2)$ is tailored with an electro-optic modulator. The temporal envelopes of the input $I_4(0,t)$, transmitted $I_4(d,t)$, and phase-conjugate $I_3(0,t)$ signals are recorded for different polarizations of the recording beams and for different pump ratios. The delay of the pulse maximum is evaluated for the phase-conjugate and transmitted beams from their temporal profiles.

The results of the measurements are shown in Fig. 9 by solid squares for the phase-conjugate pulse and by open diamonds for the transmitted pulse for $r = 0.006$, 0.06, and 1. The error bars show the scatter of the measured data. The lines represent

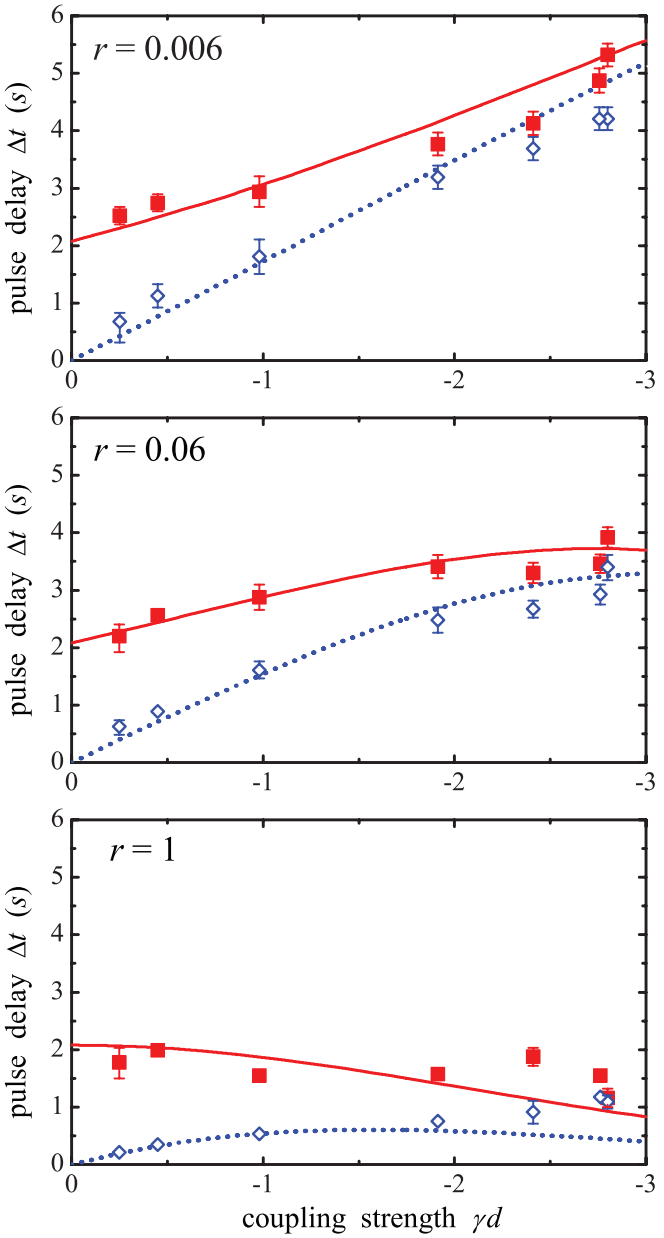

FIG. 9. (Color online) Temporal delay of maximum versus coupling strength for phase-conjugate (squares) and transmitted (diamonds) pulses, measured with $r = 0.006$, 0.06, and 1, at $\lambda = 514$ nm with total light intensity $I = 11$ W/cm^2. Lines represent calculated data shown in Fig. 3 with absolute values $\tau = 2.3$ s and $t_0 = 6.2$ s.

the calculated curves shown earlier in Fig. 3 and replotted now in absolute coordinates for $t_0 = 2.7\tau = 6.2$ s. It should be emphasized that no fitting procedure is used to generate the calculated dependencies. They are plotted for the coupling strength and grating decay time extracted for this sample from independent two-beam-coupling experiments.

IV. CONCLUSIONS

The analysis of the complex transmission and reflectivity for BWFWM with nonmonochromatic signal shows that the spectral profiles of amplitudes $A_3(\Delta\omega)$, $A_4(\Delta\omega)$, and phase $\varphi(\Delta\omega)$ depend both on the medium response time and crystal coupling strength. In this respect the response of the BWFWM differs qualitatively and quantitatively from the response of two-beam coupling: an additional factor, the coupling strength, appears for controlling the spectral shape of dispersion. This particular feature of BWFWM may manifest itself as a decrease of the nonlinear slowing down of the phase-conjugate pulse with increasing nonlinear coupling strength. The numerical calculations confirm such a nontrivial behavior: the values of the coupling strength and pump ratio are established for which the nonlinear pulse delay decreases with coupling constant. Moreover, the conditions are found for switching from pulse deceleration to pulse acceleration when the value of the coupling constant is increased.

The experimental results confirm two important theoretical predictions. First, the delay of the phase-conjugate pulse is nonzero at low coupling strength $\gamma d \to 0$. It is almost independent of the pump ratio and tends to the response time of the medium for long input pulses. Second, the tendency for a decrease of the delay with increasing magnitude of coupling strength is clearly observed at large pump-beam ratios.

It is demonstrated also that the BWFWM ensures longer pulse delay as compared with two-beam coupling for relatively modest but quite commonly used values of the coupling constant $|\gamma d| = 1$ to 3 at small pump beam ratio.

ACKNOWLEDGMENTS

K. Shcherbin cordially thanks his colleagues from ICB for their hospitality during his stay as an invited professor at Université de Bourgogne. The authors are grateful to Dr. Daniel Rytz for providing the cobalt-doped $BaTiO_3$ sample.

[1] A. Sommerfeld, Phys. Z. **8**, 841 (1907).
[2] L. Brillouin, *Wave Propagation and Group Velocity* (Academic Press, New York, 1960).
[3] A. Kasapi, M. Jain, G. Y. Yin, and S. E. Harris, Phys. Rev. Lett. **74**, 2447 (1995).
[4] L. V. Hau, S. E. Harris, Z. Dutton, and C. Behroozi, Nature (London) **397**, 594 (1999).
[5] R. W. Boyd, J. Mod. Opt. **56**, 1908 (2009).
[6] *Slow Light: Science and Applications*, edited by J. B. Khurgin and R. S. Tucker (CRC Press, Boca Raton, Fl, 2009).
[7] Y. Okawachi, M. S. Bigelow, J. E. Sharping, Z. Zhu, A. Schweinsberg, D. J. Gauthier, R. W. Boyd, and A. L. Gaeta, Phys. Rev. Lett. **94**, 153902 (2005).
[8] Z. Shi, R. W. Boyd, R. M. Camacho, Praveen K. Vudyasetu, and J. C. Howell, Phys. Rev. Lett. **99**, 240801 (2007).
[9] Y. Zhang, H. Tian, X. Zhang, N. Wang, J. Zhang, H. Wu, and P. Yuan, Opt. Lett. **35**, 691 (2010).
[10] W. Xue, S. Sales, J. Capmany, and J. Mørk, Opt. Lett. **34**, 929 (2009).
[11] P. Siddons, N. C. Bell, Y. Cai, C. S. Adams, and I. G. Hughes, Nat. Photonics **3**, 225 (2009).
[12] R. W. Boyd, J. Opt. Soc. Am. B **28**, A38 (2011).
[13] E. Podivilov, B. Sturman, A. Shumelyuk, and S. Odoulov, Phys. Rev. Lett. **91**, 083902 (2003).
[14] S. Residori, U. Bortolozzo, and J. P. Huignard, Appl. Phys. B **95**, 551 (2009).
[15] G. Zhang, F. Bo, R. Dong, and J. Xu, Phys. Rev. Lett. **93**, 133903 (2004).
[16] W. Horn, J. V. Bassewitz, and C. Denz, J. Opt. **12**, 104011 (2010).
[17] A. L. Smirl, G. C. Valley, K. M. Bohnert, and T. F. Boggess, Jr., IEEE J. Quant. Electron. **24**, 289 (1988).
[18] K. Jarasiunas, Ph. Delaye, and G. Roosen, Phys. Status Solidi B **175**, 445 (1993).
[19] U. Bortolozzo, S. Residori, and J. P. Huignard, Opt. Lett. **35**, 2076 (2010).
[20] H. N. Yum, M. Saliot, G. S. Pati, S. Tseng, P. R. Hemmer, and M. S. Shahriar, Opt. Express **16**, 20448 (2008).
[21] B. Sturman, E. Podivilov, and M. Gorkunov, Appl. Phys. B **95**, 545 (2009).
[22] B. Sturman, P. Mathey, R. Rebhi, and H.-R. Jauslin, J. Opt. Soc. B **26**, 1949 (2009).
[23] P. Mathey, G. Gadret, and K. Shcherbin, Appl. Phys. B **102**, 539 (2011).
[24] P. Mathey, G. Gadret, and K. Shcherbin, Phys. Rev. A **84**, 063802 (2011).
[25] B. Fischer, M. Cronin-Golomb, J. O. White, and A. Yariv, Opt. Lett. **6**, 519 (1981).
[26] K. R. MacDonald and J. Feinberg, Phys. Rev. Lett. **55**, 821 (1985).
[27] G. C. Papen, B. E. A. Saleh, and J. A. Tataronis, J. Opt. Soc. B **5**, 1763 (1988).
[28] R. W. Hellwarth, J. Opt. Soc. Am. **67**, 1 (1977).
[29] A. Yariv and D. M. Pepper, Opt. Lett. **1**, 16 (1977).
[30] M. Cronin-Golomb, B. Fischer, J. O. White, and A. Yariv, IEEE J. Quantum Electron. **20**, 12 (1984).
[31] J. W. S. Rayleigh, *The Theory of Sound*, (Macmillan and Co., London, 1877), Vol. I.
[32] K. R. MacDonald and J. Feinberg, J. Opt. Soc. Am. **73**, 548 (1983).